SO2 Absorption in EmimCl-TEG Deep Eutectic Solvents

Journal:	*Physical Chemistry Chemical Physics*
Manuscript ID	CP-ART-04-2018-002250.R1
Article Type:	Paper
Date Submitted by the Author:	29-Apr-2018
Complete List of Authors:	Yang, Dezhong; China University of Geosciences Beijing, School of Science Zhang, Shaoze; East China Univeristy of Science and Technology, Department of Chemistry Shanghai, CN 200237 Jiang, De-en; University of California, Riverside, Department of Chemistry Dai, Sheng; Oak Ridge National Laboratory,

Journal Name

ARTICLE

SO_2 Absorption in EmimCl-TEG Deep Eutectic Solvents

Dezhong Yang,*[a] Shaoze Zhang, [b,c] De-en Jiang,*[c] Sheng Dai,*[d,e]

Received 00th January 20xx,
Accepted 00th January 20xx

DOI: 10.1039/x0xx00000x

www.rsc.org/

Deep eutectic solvents (DESs) based on 1-ethyl-3-methylimidazolium chloride(EmimCl) and triethylene glycol (TEG) with different molar ratios (from 6:1 to 1:1) were prepared. FTIR and theoretical calculation indicated that the C_2-H on the imidazolium ring form hydrogen bonds with the hydroxyl group rather than the ether O atom of the TEG. The EmimCl-TEG DESs can efficiently capture SO_2; in particular, EmimCl-TEG (6:1) can capture 0.54g SO_2 per gram of solvent at 0.10 atm and 20 °C, the highest absorption amount for DESs at the same condition. Theoretical calculation showed that the high SO_2 absorption capacity was mainly due to the strong charge-transfer interaction between SO_2 and anion Cl^-. Moreover, SO_2 desorption in the DESs can be controlled by tuning the interaction between EmimCl and TEG, and the DESs can be cycled many times. .

Introduction

Sulfur dioxide (SO_2), as a main air contaminant, generated mainly by the combustion of fossil fuels, has destructive effects on human health and the environment.[1] Up to now, several industrial flue gas desulfurization methods have been used to control SO_2 emission. Among them, lime-limestone process is the utmost used technology on SO_2 removal. However, the lime-limestone method has some inherent shortcomings, such as the waste of water, equipment corrosion and production of solid by-product waste ($CaSO_4$). The ammonia scrubbing technology suffers the second pollution to the environment due to the volatilization of the absorbents and the seawater FGD process also have several drawbacks ,such as space requirements and large amount of seawater required. Moreover, the useful raw material SO_2 can not be recycled in the technological FGD processes mentioned above. Accordingly, it is necessary to develop reversible, economical processes for SO_2 capture.

In recent years, ionic liquids (ILs) have been widely studied for use in SO_2 capture because of their unique properties, such as high thermal stability, negligible vapor pressure and tunable structures.[6] Several anion functionalized ILs, such as azole-based and nitrile-based (thiocyanate, dicyanamide, tricyanomethanide) ILs, have be used to capture acid gas CO_2. [7,8]Han *et al.* first reported the SO_2 absorption by an IL in 2004.[9] Subsequently, a number of ILs were developed for efficient and reversible SO_2 capture. [10-16] Among them, amine-functionalized [17-19] and azole-based ILs [20-21] werediscovered that have a high SO_2 absorption capacity as a result of the multiple-site interactions between SO_2 and functional groups in the ILs. However, these functional ILs must be prepared by tedious procedures, which limits their practical application.

Recently, deep eutectic solvents (DESs) have gained much attention from researchers in many fields because of their excellent properties. [22-23] DESs can be easily obtained at high purity by mixing two or more components at suitable conditions. The melting point of the DESs is lower than those of components in the mixture because of the intermolecular hydrogen bonds formed between the components. [24-25] DESs have been studied in many fields including material chemistry, extraction, biotransformation and catalytic reactions.[26-29] Moreover, several DESs,[30-35]such as choline chloride(ChCl)-glycerol, [36] imidazole-glycerol [37]and ChCl-ethylene glycol(EG) [38]systems have been used to capture SO_2. The results showed that these DESs mentioned above are promising absorbents for SO_2 absorption. Recently, we reported that EmimCl-EG DESs can efficiently capture SO_2 with a high absorption capacity. [39]However, due to the low SO_2 concentration in flue gas, it remains challenging to design new DESs to improve their SO_2 absorption capacity at low SO_2 partial pressure.

Herein, we studied the SO_2 absorption by DESs formed by a common IL EmimCl and triethylene glycol (TEG). EmimCl is solid and TEG is liquid at room temperature. The intermolecular hydrogen bonds formed between EmimCl and TEG were studied by FTIR and theoretical calculation. The results implied that the C_2-H on the imidazolium ring mainly formed hydrogen bonds with the O atom from the hydroxyl group rather than with the ether O atom in the TEG. The rates of SO_2 solubility in EmimCl-TEG DESs with different EmimCl-TEG molar ratios(from 6:1 to 1:1) were determined. It was

---

[a] *School of Science, China University of Geosciences, Beijing 100083, China*
[b] *Key Laboratory for Advanced Materials and School of Chemistry & Molecular Engineering, East China University of Science and Technology, Shanghai 200237, China.*
[c] *Department of Chemistry, University of California, Riverside, California 92521, United States*
[d] *Chemical Sciences Division, Oak Ridge National Laboratory, Oak Ridge, Tennessee 37831, United States*
[e] *Department of Chemistry, University of Tennessee, Knoxville, Tennessee 37996, United States.*
† Email: yangdz@cugb.edu.cn; djiang@ucr.edu; dais@ornl.gov.

Electronic Supplementary Information (ESI) available: [FTIR spectra of EmimCl-TEG(4:1), EmimCl-TEG(2:1)and EmimCl-TEG(1:1) before and after SO_2 absorption]. See DOI: 10.1039/x0xx00000x demonstrated that the interaction between SO_2 and DESs can be tuned by tuning the hydrogen bonds formed between EmimCl and TEG. Moreover, the SO_2 absorption capacity of EmimCl-TEG(6:1) was 0.54 g of SO_2 per gram of solvent at 0.10 atm and 20℃,a much higher capacity than other DESs offer at the same conditions. The high SO_2 absorption capacity is due mainly to the strong charge-transfer interaction between SO_2 and the anion Cl^-.

Experimental

Materials and Characterizations

EmimCl(98%) and Triethylene glycol (98%) were purchased from Alfa Aesar. SO_2 (99.98 %) was purchased from AirGas USA. The infrared spectra were recorded on a Perkin-Elmer Frontier FTIR spectrometer (650 to 4000 cm^{-1}).

Synthesis of the DESs

DESs were prepared simply by stirring the EmimCl and TEG mixture at the desired molar ratio at 70°C until a homogeneous liquid formed. The liquids were dried under vacuum for 6 h at 60°C before use.

Absorption and desorption of SO_2

DES (about 1.0 g) was charged into a glass tube with an inner diameter of 10 mm, and the glass tube was immersed in a water or oil bath of the desired temperature. SO_2 was bubbled through the solvent in the tube at a flow rate of 50 mL/min. The amount of SO_2 absorbed by the solvent was determined at regular intervals during the absorption process by an electronic balance with an accuracy of ±0.1 mg (Mettler Toledo XS204). The method described was also used for the absorption of SO_2 under reduced partial pressure. For SO_2 absorption at different partial pressures, the SO_2 pressure was obtained by controlling the flow rates of SO_2 and N_2.

In the regeneration process, N_2 (80 mL/min) at atmospheric pressure was bubbled through the solutions at the desired temperature. The desorption temperature for EmimCl-TEG(6:1), EmimCl-TEG(4:1), and EmimCl-TEG(2:1) was 100℃. The desorption temperature for EmimCl-TEG(1:1) was 80 ℃.

Computational methodology

All calculations were carried out with the Gaussian 09 suite of programs. [40] The geometries of all the complexes under study were fully optimized by utilizing the M06-2x methods which proved to be reliable in the description of various types of noncovalent interactions.[41] Dunning's aug-cc-pVDZ basis sets were employed for all the atoms. [42] No symmetry or geometry constraint was imposed during the optimizations. All the optimized-geometries were confirmed to be local minima by means of frequency calculation at the same theoretical level. To correct for the basis set superposition error (BSSE), the standard counterpoise method of Boys and Bernardi was used. [43]

The electrostatic potential (ESP) surface maps were visualized by utilizing the Molekel 4.3 program.[44] The interaction energy (ΔE) between solvent and gas was evaluated as

$$\Delta E = E_{system} - E_{solvent} - nE_{SO_2},$$

where E_{system} is the energy of the optimized system containing both the solvent and the gas molecules, $E_{solvent}$ is the energy of the solvent, n is the number of SO_2 gas molecules in the system, and E_{SO2} is a gas-phase SO_2 molecule.

Results and discussion

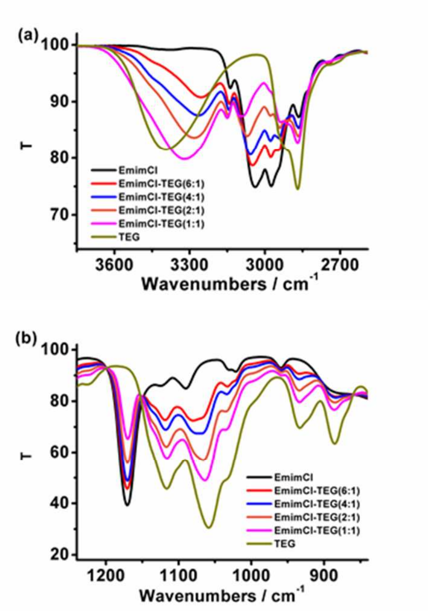

Fig.1 FTIR spectra of EmimCl, EmimCl-TEG DESs and TEG.

EmimCl and TEG can form DESs at room temperature mainly because of intermolecular hydrogen bonding between EmimCl and TEG. The hydrogen bonding between EmimCl and TEG was investigated by Fourier transform infrared (FTIR) spectroscopy (Fig.1). The EmimCl spectrum was obtained when EmimCl was in molten state. As shown in Fig. 1a, the hydroxyl (O-H) stretching peak in pure TEG was at 3395 cm^{-1}. The O-H stretching in the DESs EmimCl-TEG(1:1) shifted to a lower wavenumber, appearing at 3321 cm^{-1} . Moreover, as the EmimCl concentrations in the DESs increased, the O-H stretching band decreased continuously to lower wavenumbers. This peak appeared at 3254 cm^{-1} in the EmimCl-TEG(6:1) system and the red shift was 141cm^{-1}(Table S1), indicating strong hydrogen bonding interaction between the OH group of TEG and EmimCl.[45-46]

In pure EmimCl, the imidazolium ring C-H stretching vibration appeared at 3038 cm^{-1} for C_2-H and 3139 cm^{-1} for $C_{4,5}$-H.[47] As seen in Fig. 1a, the EmimCl ring C-H stretching modes moved to higher wavenumbers continuously as the TEG concentration in the solvents increased. The blue shift of the ring C-H can probably be attributed to two causes. One is that the hydrogen bonding interaction between the ring C-H and Cl^- (C-H⋯Cl^-) was reduced by the formation of hydrogen bonds between Cl^- and OH (OH⋯Cl^-) of the TEG. As is presented in other work, the imidazolium ring C-H stretching bond would shift to lower wavenumbers for stronger interacting anions.[48] In other words, the ring C-H stretching bond should shift to higher wavenumbers as the interaction between C-H and anion is reduced. The other cause is the formation of hydrogen bonds between the ring C-H and the O atom (C-H⋯O) of TEG. The ring $C_{4,5}$-H stretching peaks in EmimCl-TEG(1:1) (3151 cm^{-1}) were blue-shifted by 12 cm^{-1} compared with that in the pure IL (3139 cm^{-1}). However, C_2-H peaks moved from 3038 (EmimCl) to 3094 cm^{-1} (EmimCl-TEG(1:1)), showing a 56 cm^{-1} blue shift, as seen in Fig. 1a. The C_2-H showed a bigger blue shift than the $C_{4,5}$-H, suggesting that C_2-H is more likely to form hydrogen bonds with O atoms. This result is inconsistent with those in other reports.[49-50] It occurs because the C_2-H is more acidic than $C_{4,5}$-H. [51]There are two kinds of O atoms in TEG: the O of the OH group and O atom of ether. Are they equal when they forming hydrogen bonds with the H on the imidazolium ring? As can be seen in Fig. 1b, the C-OH stretching vibration bonds of TEG shifted from 1059 (TEG) to 1080 cm^{-1} (EmimCl-TEG[6:1]) and C-O-C stretching peaks shifted from 1116(TEG) to 1119 cm^{-1} (EmimCl-TEG[6:1]). [52]The C-OH showed a much bigger shift (21 cm^{-1}) than C-O-C(3 cm^{-1}), implying that the hydrogen bond C_2-H···OH arrangement was preferred over C_2-H···O-ether.

The interactions between EmimCl and TEG in the four DESs systems were further studied by the theoretical calculation. The optimized structures showing the interactions between EmimCl and TEG in the four DESs are shown in Fig. 2. As can be seen in Fig. 2, the hydrogen bonds between EmimCl and TEG are mainly formed by the C_2-H on the imidazolium with OH group of TEG (C_2-H···OH) and anion Cl^- with hydrogen in OH group (OH···Cl^-) . The calculation results are in consistent with the experimental results. Moreover, it is interesting that TEG in EmimCl-TEG(1:1) system is in twisted conformation rather than straight-chain conformation and the two OH groups interact simultaneously with Cl^-.

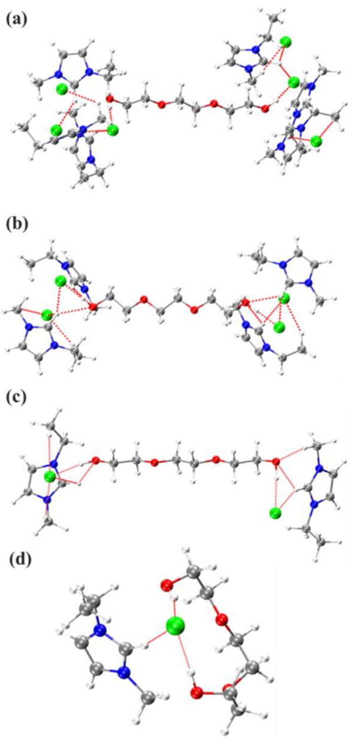

Fig. 2 Hydrogen bonds in different EmimCl-TEG DESs: a) EmimCl-TEG (6:1); b) EmimCl-TEG(4:1); c) EmimCl-TEG(2:1); d) EmimCl-TEG(1:1). C, grey; N, blue; O, red; H, white; Cl, green

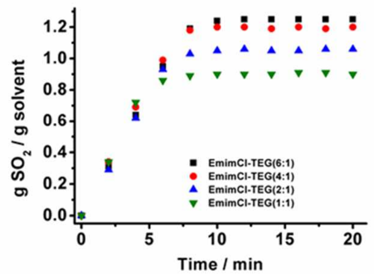

Fig.3 Comparison of SO_2 absorption by EmimCl-TEG DESs as a function of time at 20°C and 1.0 atm.

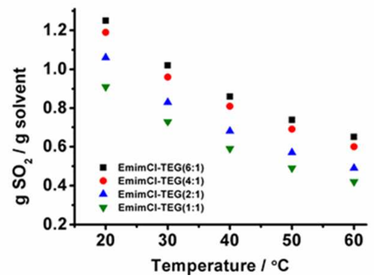

Fig.4 Effect of temperature on SO_2 absorption by EmimCl-TEG DESs at 1.0 atm.

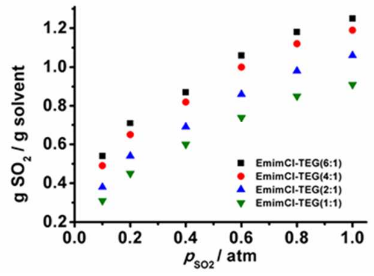

Fig. 5 Effect of pressure on SO_2 absorption by EmimCl-TEG at 20°C.

Fig. 3 shows the SO_2 absorption of the solvents at 20℃ and 1.0 atm as the function of time. As can be seen in Fig. 3, the SO_2 absorption capacity of EmimCl-TEG(6:1) reached 1.25 g SO_2/ g solvent, which is extremely high. This is mainly because of the strong charge-transfer interaction between SO_2 and the anion Cl^- in the solvent.[16, 53-54]Moreover, the SO_2 absorption capacities of the DESs decreased as the concentration of EmimCl decreased in the solvents, implying that the EmimCl played an important role in improving the SO_2 absorption capacity of DESs.

The effect of temperature on the SO_2 absorption of the solvent is shown in Fig. 4. It can be seen that the SO_2 absorption capacities of the solvents decreased as the temperature increased. For example, as the temperature increased from 20 to 60℃, the amount of SO_2 absorbed by EmimCl-TEG(6:1) and EmimCl-TEG(4:1) decreased from 1.25 to 0.65 g SO_2/ g solvent and from 1.20 to 0.61 g SO_2/ g solvent, repectively, indicating that the low temperatures are beneficial for SO_2 absorption by DESs.

Fig. 5 shows the effect of SO_2 pressure on the absorption capacity of the DESs at 20℃. According to Fig. 5, the SO_2 absorption capacities of the solvents increased with increasing SO_2 partial pressure. The SO_2 absorption capacity of EmimCl-TEG(6:1) increased from 0.54 to 1.25 g SO_2/g solvent as the SO_2 partial pressure changed from 0.10 to 1.0 atm.

The SO_2 uptake rates of the four DESs were compared with those of other DESs and ILs, as shown in Table 1. As shown, the EmimCl-TEG(6:1) has the extremely high SO_2 absorption capacity at

Table 1. Comparison of SO_2 absorption capacities of different DESs and ILs

		SO_2 absorption [g SO_2 / g solvent]		
IL or DES	T/°C	1.0 atm	0.10 atm	Reference
EmimCl-TEG (6:1)	20	1.25	0.54	This work
EmimCl-TEG (4:1)	20	1.20	0.50	This work
EmimCl-EG (2:1)	20	1.15	0.42	39
EmimCl-TEG (2:1)	20	1.06	0.38	This work
[Emim][SCN]	20	1.13	0.37	15
$[NEt_2C_2Py][SCN]$	20	1.06	0.37	19
ACC-Im(1:2)	30	0.989	0.381	35
EmimCl-TEG (1:1)	20	0.91	0.31	This work
Im-Glycerol (1:2)	40	—	0.253^a	37
ChCl-Thiourea (1:1)	30	0.70	0.09^b	38
ChCl-Glycerol(1:1)	20	0.678	0.153	36
CPL-KSCN(3:1)	20	0.607	—	31
ChCl-LA(1:3)	20	0.557	0.124	34
ChCl-EG (1:2)	30	0.55	0.16^b	38
$[P_{66614}][Tetz]$	20	0.43	0.18	20
Bet-EG(1:3)	40	0.366	0.0701^a	33
L-car-EG(1:3)	40	0.365	0.151^a	33

^{a}At 0.02 atm. ^{b}At 0.20 atm.

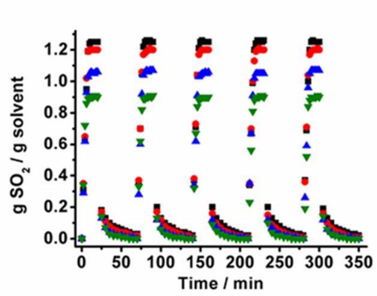

Fig. 6 SO_2 absorption-desorption cycles of EmimCl-TEG DESs: ■=(6:1), ●=(4:1), ▲=(2:1), ▼=(1:1).

both 1.0 and 0.10 atm. EmimCl-TEG(6:1) could capture as much as 0.54 g SO_2/ g solvent at 0.10 atm. To the best of our knowledge, this value is the highest absorption ratio by DESs at those conditions reported to date. This is a great advance because of the low SO_2 concentration in flue gas. It is crucial to improve the SO_2 absorption capacity of solvents at low SO_2 partial pressures for industrial applications. However, EmimCl and EG could not form liquid mixture with the ratio of 6:1 at room temperature. So, at this point, EmimCl-TEG DESs are in a more advantageous position than the Emim-EG system for SO_2 absorption .In this work, we also studied the reusability of the DESs, because absorbent recyclability is important for an efficient SO_2 capture process. The absorption-desorption processes are illustrated in Fig. 6. Most SO_2 (～98%) captured by EmimCl-TEG(6:1) was desorbed at 100℃ in 50 min by bubbling N_2 through the solvent. Nearly all the absorbed SO_2 (> 99%) was released by the EmimCl-TEG(2:1) solvent at the same condition. Furthermore, all the SO_2 captured by EmimCl-TEG(1:1) can be desorbed at 80 ℃ within 50 min. The different desorption behaviors are due mainly to tuning the interaction between SO_2 and Cl^-, which is discussed in the following section.

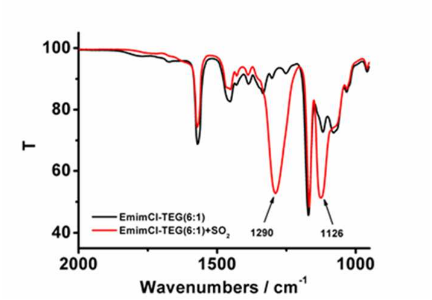

Fig. 7 FTIR spectrum for EmimCl-TEG(6:1) before and after SO_2 absorption

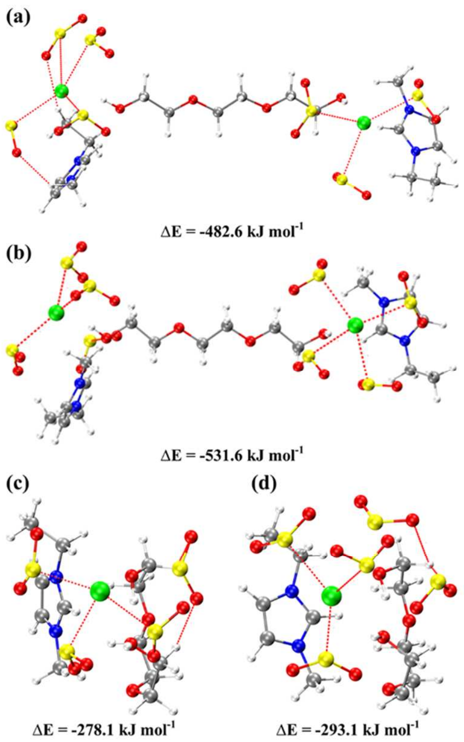

Fig. 8 Optimized structures showing interactions between the EmimCl-TEG DESs and SO_2: a) EmimCl-TEG(2:1)+7SO_2; b) EmimCl-TEG(2:1)+8SO_2; c) EmimCl-TEG(1:1)+4SO_2; d) EmimCl-TEG(1:1)+5SO_2. The interaction energy, Δ*E*, between the solvent components and the SO_2 gas molecules, is also given for each case. S, yellow; O, red; C, grey; N, blue; H, white; Cl, green

To study the interaction between SO_2 and the DESs, we analyzed the FTIR of EmimCl-TEG(6:1) before and after SO_2 absorption. Compared the FTIR spectra before and after SO_2 absorption (Fig. 7), two new peaks, the asymmetrical (V_{as}) and symmetrical (V_s) stretching vibration of SO_2 centered at 1290 and 1126 cm^{-1}, respectively, were found. However, these stretching bands appeared at 1344 (V_{as}) and 1145 cm^{-1} (V_s) for SO_2 in CCl_4, [55]and we found that the V_{as} peak of SO_2 in TEG was at 1324 cm^{-1}. Thus, the asymmetrical band of SO_2 shifted to lower wavenumbers after SO_2 was captured in EmimCl- TEG(6:1); this shift was mainly because of the strong charge-transfer interaction between the sulfur atom of SO_2 and the Cl^-. Moreover, the V_{as} peaks of the absorbed SO_2 in EmimCl-TEG(4:1), EmimCl-TEG(2:1) and EmimCl-TEG(1:1), appeared at 1294 (Fig. S1), 1303 (Fig. S2) and 1309 cm^{-1} (Fig. S3), respectively. In other words, the asymmetrical bands of SO_2 moved continuously to higher wavenumbers as the TEG concentration increased in DESs. These results indicated that the interactions between SO_2 and Cl^- were reduced with increasing concentration of TEG in DESs, which is favorable for SO_2 desorption.

This is mainly because of a higher level of TEG in the DESs strengths hydrogen bonding between the OH of TEG and Cl^-, causing the interaction between SO_2 and Cl^- to be reduced. These results are inconsistent with the SO_2 desorption behavior of the DESs.

To further study the interaction between SO_2 and DESs, theoretical investigation was conducted to optimize the interaction geometries and obtain the interaction energetics. Based on the experimental results, the molar ratios of EmimCl:TEG:SO_2 were 2:1:7.3 and 1:1:4.2 for EmimCl-TEG(2:1) and EmimCl-TEG(1:1) systems, respectively, under saturation conditions at 20℃ and 1.0 atm. Thus, the optimized structures of EmimCl-TEG(2:1)+7SO_2, EmimCl-TEG(2:1)+8SO_2, EmimCl-TEG(1:1)+4SO_2 and EmimCl-TEG(1:1)+5SO_2 were calculated and the results are shown in Fig. 8. As shown in Fig. 8, SO_2 mainly interacted with the anion Cl^- in the DESs. We also calculated the interaction energy (ΔE) between SO_2 and DESs. One can see that the interaction energy generally increases with the number of SO_2 molecules in the system, ranging from -278.1 kJ mol^{-1} for EmimCl-TEG(1:1)+4SO_2 to -531.6 kJ mol^{-1} for EmimCl-TEG(2:1)+8SO_2, confirming the strong interaction between SO_2 and DESs via mainly the interaction of SO_2 and Cl^-.[56]

Conclusions

The hydrogen bond interaction between EmimCl and TEG was tuned by changing the compositions of EmimCl-TEG DESs. The results indicated that the intermolecular hydrogen bond the $C_2H\cdots OH$ arrangement was preferred over $C_2H\cdots O$-ether. All the EmimCl-TEG DESs efficiently absorb SO_2 as the result of the charge transfer interaction between SO_2 and Cl^-. EmimCl-TEG(6:1) capture 0.54 g of SO_2 per gram of solvent at 0.10 atm and 20℃, a higher rate than that of other DESs at the same condition. Furthermore, the interaction between SO_2 and Cl^- was tuned by tuning the hydrogen bond between EmimCl and TEG, and all DESs showed good reversibility.

Conflicts of interest

There are no conflicts to declare.

Acknowledgements

This work was supported financially by the National Natural Science Foundation of China (No. 21503196) and the Fundamental Research Funds of the Central Universities (No. 2652015192). S. Dai was supported by the Division of Chemical Sciences, Geosciences, and Biosciences, Office of Basic Energy Sciences, US Department of Energy.

Notes and references

1 C. Vahlsing and K. R. Smith, *Air Qual., Atmos. Health*, 2012, **5**, 393-399.
2 F. Scala and P. Salatino, *Chem. Eng. Sci.*, 2010, **65**, 556-561.
3 F. J. G. Ortiz, F. Vidal, P. Ollero, L. Salvador, V. Cortes and A. Gimenez, *Ind. Eng. Chem. Res.*, 2006, **45**, 1466-1477.
4 P. Córdoba, *Fuel*, 2015, **144**, 274-286.
5 M. S. Shannon, A. C. Irvin, H. N. Liu, J. D. Moon, M. S. Hindman, C. H. Turner and J. E. Bara, *Ind. Eng. Chem. Res.*, 2015, **54**, 462-471.
6 T. Itoh, *Chem. Rev.*, 2017, **117**, 10567-10607.
7 K. M. Gupta and J. Jiang, *J Phys. Chem. C*, 2014, **118**, 3110-3118.
8 C. M. Wang, X. Y. Luo, H. M. Luo, D. E. Jiang, H. R. Li and S. Dai, *Angew. Chem. Int. Ed.*, 2011, **50**, 4918-4922.
9 W. Z. Wu, B. X. Han, H. X. Gao, Z. M. Liu, T. Jiang and J. Huang, *Angew. Chem. Int. Ed.*, 2004, **43**, 2415-2417.
10 J. L. Anderson, J. K. Dixon, E. J. Maginn and J. F. Brennecke, *J. Phys. Chem. B*, 2006, **110**, 15059-15062.
11 J. Huang, A. Riisager, P. Wasserscheid and R. Fehrmann, *Chem. Commun.*, 2006, 4027-4029.
12 S. Y. Hong, J. Im, J. Palgunadi, S. D. Lee, J. S. Lee, H. S. Kim, M. Cheong and K. D. Jung, *Energy Environ. Sci.*, 2011, **4**, 1802-1806.
13 M. J. Jin, Y. C. Hou, W. Z. Wu, S. H. Ren, S. D. Tian, L. Xiao and Z. G. Lei, *J. Phys. Chem. B*, 2011, **115**, 6585-6591.
14 G. K. Cui, J. J. Zheng, X. Y. Luo, W. J. Lin, F. Ding, H. R. Li and C. M. Wang, *Angew. Chem. Int. Ed.*, 2013, **52**, 10620-10624.
15 C. M. Wang, J. J. Zheng, G. K. Cui, X. Y. Luo, Y. Guo and H. R. Li, *Chem. Commun.*, 2013, **49**, 1166-1168.
16 K. Y. Lee, C. S. Kim, H. Kim, M. Cheong, D. K. Mukherjee and K. D. Jung, *Bull. Korean Chem. Soc.*, 2010, **31**, 1937-1940.
17 Z. Z. Yang, L. N. He, Q. W. Song, K. H. Chen, A. H. Liu and X. M. Liu, *Phys. Chem. Chem. Phys.*, 2012, **14**, 15832-15839.
18 D. Z. Yang, M. Q. Hou, H. Ning, J. Ma, X. C. Kang, J. L. Zhang and B. X. Han, *ChemSuschem*, 2013, **6**, 1191-1195.
19 S. J. Zeng, H. Y. He, H. S. Gao, X. P. Zhang, J. Wang, Y. Huang and S. J. Zhang, *RSC Adv.*, 2015, **5**, 2470-2478.
20 C. M. Wang, G. K. Cui, X. Y. Luo, Y. J. Xu, H. R. Li and S. Dai, *J. Am. Chem. Soc.*, 2011, **133**, 11916-11919.
21 G. K. Cui, C. M. Wang, J. J. Zheng, Y. Guo, X. Y. Luo and H. R. Li, *Chem. Commun.*, 2012, **48**, 2633-2635.
22 Q. H. Zhang, K. D. Vigier, S. Royer and F. Jerome, *Chem. Soc. Rev.*, 2012, **41**, 7108-7146.
23 A. Paiva, R. Craveiro, I. Aroso, M. Martins, R. L. Reis and A. R. C. Duarte, *ACS Sustainable Chem. Eng.*, 2014, **2**, 1063-1071.
24 D. V. Wagle, H. Zhao and G. A. Baker, *Acc. Chem. Res.*, 2014, **47**, 2299-2308.
25 M. Francisco, A. van den Bruinhorst and M. C. Kroon, *Angew. Chem.Int. Ed.*, 2013, **52**, 3074-3085.
26 F. Pena-Pereira and J. Namiesnik, *ChemSuschem*, 2014, **7**, 1784-1800.
27 E. L. Smith, A. P. Abbott and K. S. Ryder, *Chem. Rev.*, 2014, **114**, 11060-11082.
28 S. E. E. Warrag, C. J. Peters and M. C. Kroon, *Curr. Opin. Green Sust. Chem*, 2017, **5**, 55-60.
29 M. Ruesgas-Ramón, M. C. Figueroa-Espinoza and E. Durand, *J. Agric. Food Chem.*, 2017, **65**, 3591-3601.
30 G. Garcia, S. Aparicio, R. Ullah and M. Atilhan, *Energy Fuel*, 2015, **29**, 2616-2644.
31 B. Y. Liu, F. X. Wei, J. J. Zhao and Y. Y. Wang, *RSC Adv.*, 2013, **3**, 2470-2476.
32 B. Liu, J. Zhao and F. Wei, *J. Mol. Liq.*, 2013, **180**, 19-25.
33 K. Zhang, S. H. Ren, Y. C. Hou and W. Z. Wu, *J. Hazard. Mater.*, 2017, **324**, 457-463.
34 D. S. Deng, G. Q. Han and Y. T. Jiang, *New J Chem.*, 2015, **39**, 8158-8164.
35 D. S. Deng, X. B. Liu and B. Gao, *Ind. Eng. Chem. Res.*, 2017, **56**, 13850-13856.
36 D. Z. Yang, M. Q. Hou, H. Ning, J. L. Zhang, J. Ma, G. Y. Yang and B. X. Han, *Green Chem.*, 2013, **15**, 2261-2265.
37 K. Zhang, S. Ren, X. Yang, Y. Hou, W. Wu and Y. Bao, *Chem. Eng. J.*, 2017, **327**, 128-134.
38 S. Y. Sun, Y. X. Niu, Q. Xu, Z. C. Sun and X. H. Wei, *Ind. Eng. Chem. Res.*, 2015, **54**, 8019-8024.

39 D. Yang, Y. Han, H. Qi, Y. Wang and S. Dai, *ACS Sustainable Chem. Eng.*, 2017, **5**, 6382-6386.
40 M. T. Frisch, G.; Schlegel, H. B.; Scuseria, G.; Robb, M.; Cheeseman, J.; Scalmani, G.; Barone, V.; Mennucci, B.; Petersson, G.,, ed., Gaussian 09, revision D. 01. 2009. Gaussian, Inc., Wallingford CT:, 2009.
41 Y. Zhao and D. G. Truhlar, *Theor. Chem. Acc.*, 2008, **120**, 215-241.
42 R. A. Kendall, T. H. D. Jr. and R. J. Harrison, *J. Chem. Phys.*, 1992, **96**, 6796-6806.
43 S. F. Boys and F. Bernardi, *Mol. Phys.*, 1970, **19**, 553-566.
44 S. L. Portmann, Hans Peter, *Chimia* 2000, **54**, 766-700.
45 H. Ghaedi, M. Ayoub, S. Sufian, B. Lal and Y. Uemura, *J.Mol. Liq.*, 2017, **242**, 395-403.
46 J. Jiang, C. Yan, X. Zhao, H. Luo, Z. Xue and T. Mu, *Green Chem.*, 2017, **19**, 3023-3031.
47 S. Chatzipapadopoulos, T. Zentel, R. Ludwig, M. Lutgens, S. Lochbrunner and O. Kuhn, *ChemPhysChem*, 2015, **16**, 2519-2523.
48 V. H. Paschoal, L. F. O. Faria and M. C. C. Ribeiro, *Chem. Rev.*, 2017, **117**, 7053-7112.
49 A. Mehrdad and Z. Niknam, *J. Chem. Eng. Data*, 2016, **61**, 1700-1709.
50 M. S. Reddy, S. M. Nayeem, C. Soumini, K. T. S. S. Raju and B. H. Babu, *Thermochim. Acta*, 2016, **630**, 37-49.
51 K. X. Li, Y. B. Yan, J. Zhao, J. X. Lei, X. L. Jia, S. H. Mushrif and Y. H. Yang, *Phys. Chem. Chem. Phys.*, 2016, **18**, 32723-32734.
52 X. S. Qiao, T. X. Zhao, B. Guo, F. Sha, F. Zhang, X. H. Xie and J. B. Zhang, *J. Chem. Eng. Data*, 2016, **61**, 1597-1607.
53 R. A. Ando, L. J. A. Siqueira, F. C. Bazito, R. M. Torresi and P. S. Santos, *J. Phys. Chem. B*, 2007, **111**, 8717-8719.
54 H. B. Xing, C. Liao, Q. W. Yang, G. M. Veith, B. K. Guo, X. G. Sun, Q. L. Ren, Y. S. Hu and S. Dai, *Angew. Chem. Int. Ed.*, 2014, **53**, 2099-2103.
55 M. H. H. vanDam, A. S. Lamine, D. Roizard, P. Lochon and C. Roizard, *Ind. Eng. Chem. Res.*, 1997, **36**, 4628-4637.
56 H. Li, Y. Chang, W. Zhu, C. Wang, C. Wang, S. Yin, M. Zhang and H. Li, *Phys. Chem. Chem. Phys.*, 2015, **17**, 28729-28742.

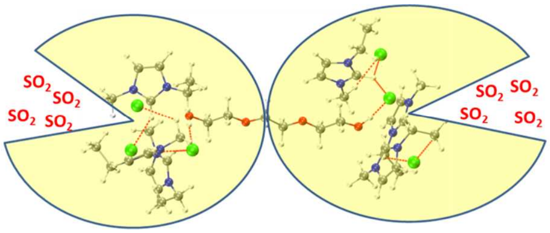

C_2-H on imidazolium ring mainly interacted with hydroxyl group of TEG, and EmimCl-TEG DESs have a high SO_2 absorption capacity.